THE JOURNAL OF BIOLOGICAL CHEMISTRY VOL. 282, NO. 3, pp. 1891–1904, January 19, 2007

The Expression of *Clcn7* and *Ostm1* in Osteoclasts Is Coregulated by Microphthalmia Transcription Factor*

Received for publication, September 6, 2006, and in revised form, November 10, 2006 Published, JBC Papers in Press, November 14, 2006, DOI 10.1074/jbc.M608572200

Nicholas A. Meadows[‡§], Sudarshana M. Sharma[¶], Geoffrey J. Faulkner[‡], Michael C. Ostrowski[¶], David A. Hume[‡§], and Alan I. Cassady[‡§1]

From the [‡]Institute for Molecular Biosciences, the University of Queensland, St. Lucia, Queensland 4072, Australia, [§]Cooperative Research Centre for Chronic Inflammatory Diseases, St. Lucia, Queensland 4072, Australia, and the [¶]Department of Molecular Genetics, Ohio State University, Columbus, Ohio 43210

Microphthalmia transcription factor (MITF) regulates osteoclast function by controling the expression of genes, including tartrate-resistant acid phosphatase (TRAP) and cathepsin K in response to receptor activator of nuclear factor-κB ligand (RANKL)-induced signaling. To identify novel MITF target genes, we have overexpressed MITF in the murine macrophage cell line RAW264.7 subclone 4 (RAW/C4) and examined the gene expression profile after sRANKL-stimulated osteoclastogenesis. Microarray analysis identified a set of genes superinduced by MITF overexpression, including *Clcn7* (chloride channel 7) and *Ostm1* (osteopetrosis-associated transmembrane protein 1). Using electrophoretic mobility shift assays, we identified two MITF-binding sites (M-boxes) in the *Clcn7* promoter and a single M-box in the *Ostm1* promoter. An anti-MITF antibody supershifted DNA-protein complexes for promoter sites in both genes, whereas MITF binding was abolished by mutation of these sites. The *Clcn7* promoter was transactivated by coexpression of MITF in reporter gene assays. Mutation of one *Clcn7* M-box prevented MITF transactivation, but mutation of the second MITF-binding site only reduced basal activity. Chromatin immunoprecipitation assays confirmed that the two *Clcn7* MITF binding and responsive regions *in vitro* bind MITF in genomic DNA. The expression of *Clcn7* is repressed in the dominant negative mutant *Mitf* mouse, *mi/mi*, indicating that the dysregulated bone resorption seen in these mice can be attributed in part to transcriptional repression of *Clcn7*. MITF regulation of the TRAP, cathepsin K, *Clcn7*, and *Ostm1* genes, which are critical for osteoclast resorption, suggests that the role of MITF is more significant than previously perceived and that MITF may be a master regulator of osteoclast function and bone resorption.

Bone-resorbing osteoclasts are multinucleated cells that are derived from the hematopoietic myeloid/monocyte lineage. Normal bone remodeling is controlled by the close interactions between osteoclasts and osteoblasts, the primary bone-synthesizing cells. The balance between the activities of these two cell types is controlled by tight transcriptional regulation of both osteoclast-specific and osteoblast-specific genes along with signaling mechanisms that couple the actions of these cells. Defects in the transcriptional control of osteoclasts can result in a failure of either cell differentiation or function. The resulting loss of bone resorption results in the development of osteopetrosis, a condition characterized by dense brittle bones and the lack of a marrow cavity. The use of transgenic gene knock-out mice has elucidated the role of several transcription factors in regulating osteoclast differentiation and function. Null mutations in *PU.1* (1), c-*Fos* (2), and *NF-κB* p50/p52 (3–5) all result in osteopetrosis, thereby indicating that these transcription factors play a critical role in regulating osteoclast biology.

Microphthalmia transcription factor (MITF)[2] has been shown to be a regulator of osteoclast function by activating transcription of the osteoclast-overexpressed genes, TRAP and cathepsin K (6, 7). MITF is a member of the basic helix-loop-helix-leucine zipper (b-HLH-ZIP) family of transcription factors. This family is defined by the presence of a DNA-binding basic region, the HLH motif, and the protein association leucine zipper domain motif (8). Together with TFEB, TFEC, and TFE3, MITF forms part of the MiT (Mitf-TFE) subgroup of the b-HLH-ZIP family. These MiT factors form homodimers and heterodimers with each other but do not heterodimerize with b-HLH-ZIP factors of other subfamilies (9). All MiT factors are expressed in cells of the mononuclear phagocyte lineage with TFE3 and TFEB being widely expressed in other cell types but TFEC being restricted to myeloid cells (10).

Homozygous loss-of-function or deletion mutations of *Mitf* in the mouse result in an absence of coat pigmentation, deafness, and microphthalmia (8). Homozygous semi-dominant mutations in *Mitf* affect cell types, including osteoclasts, mast cells, and NK cells (8). Heterozygous mutations of the *Mitf* gene

* This work was supported by the National Health and Medical Research Council Grant 210261 and by the Cooperative Research Centre for Chronic Inflammatory Diseases, Australia. The costs of publication of this article were defrayed in part by the payment of page charges. This article must therefore be hereby marked "*advertisement*" in accordance with 18 U.S.C. Section 1734 solely to indicate this fact.

[1] To whom correspondence should be addressed. Tel.: 61-7-3346-2076; Fax: 61-7-3346-2101; E-mail: I.Cassady@imb.uq.edu.au.

[2] The abbreviations used are: MITF, microphthalmia transcription factor; PIPES, 1,4-piperazinediethanesulfonic acid; eGFP, enhanced green fluorescent protein; PBS, phosphate-buffered saline; DTT, dithiothreitol; PMSF, phenylmethylsulfonyl fluoride; b-HLH-ZIP, basic helix-loop-helix-leucine zipper; DAPI, 4,6-diamidino-2-phenylindole; OCL, osteoclast-like cells; EMSA, electrophoretic mobility shift assays; TEMED, *N*,*N*′,*N*′-tetramethylethylenediamine; TRAP, tartrate-resistant acid phosphatase; qPCR, quantitative real time PCR; ChIP, chromatin immunoprecipitation; RANK, receptor activator of nuclear factor-κB; sRANKL, soluble recombinant human receptor activator of nuclear factor-κB ligand; oligo, oligonucleotide; MAP, mitogen-activated protein.

in humans result in Waardenburg syndrome type 2a (11) and Tietz syndrome (12), which are characterized by deafness and hypopigmentation of the hair, skin, and iris.

The *mi* mutant allele of *Mitf* has a 3-bpr deletion, which removes one of four arginine residues in the basic region that are necessary for MITF binding to DNA (9, 13). As a result, the *mi/mi* mouse has a severe defect in osteoclast maturation that produces profound osteopetrosis. This is characterized by the lack of a ruffled border, failure to fuse in order to form multinucleated cells, and ultimately a defect in bone resorption (14, 15). The osteopetrotic defect in the *mi/mi* mice therefore results from deficiencies in the terminal differentiation and function of osteoclasts and differs from other osteopetrotic mouse defects, including null mutations of *PU.1*, *c-Fos*, and *NF-κB*, in which earlier stages of osteoclast differentiation are affected (1–4).

The activation of MITF in osteoclasts via the phosphorylation of serine residues is dependent on TRAF6-mediated signaling in response to RANKL binding to its receptor, RANK (16). Site-directed alanine substitution of Ser-73 or Ser-409 results in transcriptionally inactive MITF, and these residues are targets of phosphorylation by MAP kinase and RSK-1 (17, 18). In osteoclasts, MITF has been identified as a target of Ser-307 phosphorylation by p38 MAP kinase in response to RANKL treatment (19).

Transcriptional targets of MITF have been identified at cellular sites where the mutant alleles generate a phenotypic change, including the following: pigment cells, mast cells, and osteoclasts. Pigment cell-specific genes include the following: tyrosinase (Tyr) and tyrosine-related genes, *Tyrp1* and *Dct/Tyrp2* (20); melanocortin-1 receptor (21); T-box protein 2 (22); *QNR-71* (23); *silver* (24); *absent in melanoma 1* (25); and B cell leukemia/lymphoma 2 (26). Mast cell-specific genes include the following: mast cell proteases 2, 4, 5, 6, and 9 (27–31); granzyme B and tryptophan hydroxylase (32); c-*kit* (33); nerve growth factor receptor (34); *SgIGSF* (35); *NDST-2* (36); integrin α4 (37); *Bcl-2* (26); and *PAI-1* (38). Osteoclast-specific genes include the following: tartrate-resistant acid phosphatase (TRAP) (6); cathepsin K (7); *OSCAR* (39); and E-cadherin (40).

Our aim is the systematic identification of MITF transcriptional target genes in osteoclasts. We propose that this will provide a unique insight into mature osteoclast function, in particular the transcriptional regulation of genes associated with osteoclastic bone resorption. To determine the role of MITF in mature osteoclast function, we identified genes with high expression in osteoclast-like cells late in the differentiation process. One such gene is *Clcn7* (chloride channel 7), which is the major chloride channel expressed in the ruffled border of the mature osteoclast (41). The expression of *Clcn7* was also affected in cells with dysregulated levels of MITF protein. Disruption of CLCN7 activity leads to severe osteopetrosis in mice and humans because of a failure of the osteoclast to secrete acid (41, 42).

The grey-lethal (*gl*) murine and human alleles contain a mutation in the *Ostm1* gene and are characterized by severe osteopetrosis (43). The OSTM1 protein forms a complex with CLCN7 and as such has been proposed to be a β-subunit of active CLCN7 (44). The osteopetrotic phenotype associated with *Ostm1* mutations may result from the impairment of CLCN7-dependent acidification of the osteoclast resorption lacuna (44).

In this study, we report several lines of evidence that MITF regulates both the *Clcn7* and *Ostm1* genes during osteoclast maturation. In particular, reporter gene assays using transfection of osteoclast-like cells (OCL) coupled with electrophoretic mobility shift assays provide strong evidence of MITF regulation of the *Clcn7* and *Ostm1* promoters, and chromatin immunoprecipitation assays validate MITF binding to the *Clcn7* promoter. This study also shows that *Clcn7* mRNA expression is repressed in primary osteoclasts derived from *mi/mi* mice and up-regulated in OCL overexpressing MITF protein. Our observation that MITF controls the expression of *Clcn7* and *Ostm1* along with TRAP and cathepsin K suggests that MITF is in fact a master regulator of a set of genes required for osteoclast function and bone resorption.

EXPERIMENTAL PROCEDURES

Materials—We used the following: G418 (geneticin) (Sigma); the cytokines used were soluble recombinant human RANKL (sRANKL) (PeproTech) and human colony-stimulating factor-1 (a gift from Chiron Corp., Emeryville, CA); the plasmids used were pEF6 (Invitrogen), pGL2-Basic (Promega, Madison, WI), and pEGFP-1 (Clontech); the cell lines used were RAW/C4 cells, a subclone of the RAW264.7 macrophage-like cell line (ATCC, Manassas, VA (45)); the antibodies used were mouse anti-V5 antibody (Serotec, Oxford, UK), horseradish peroxidase-conjugated anti-mouse antibody (Cell Signaling Technology, Inc. Beverly, MA), goat anti-mouse phycoerythrin antibody (Molecular Probes), and mouse monoclonal anti-MITF antibody (NeoMarkers, Freemont, CA). Mice heterozygous for the *mi* mutation (B6C3Fe background) were obtained originally from The Jackson Laboratory (Bar Harbor, ME).

Generation of RAW/C4 Cell Lines Stably Transfected with an MITF Expression Construct and a TRAP Promoter-eGFP Reporter—The coding region of the wild type murine *Mitf*-A isoform was PCR-amplified using the following primers: sense primer (5′-CGG GTT CTG GTC CAA GTC CCA AGC AG-3′) and antisense primer (5′-ACA CGC ATG CTC CGT TTC TTC-3′) with the *Mitf*-pECE construct as the template. The PCR product was cloned into the pEF6/V5-His TOPO TA vector (Invitrogen). A murine 620-bp TRAP promoter-eGFP reporter construct, described previously, was used to monitor the activity of the exogenous proteins (6, 46).

RAW/C4 cells were cultured in Dulbecco's modified Eagle's medium (Invitrogen) containing 4 mM L-glutamine, 50 μg/ml penicillin, 50 μg/ml streptomycin (Invitrogen), and 5% heat-inactivated fetal calf serum (Serum Supreme; BioWhittaker, Walkersville, MD). The cells were plated at a density of 3×10^5 cells/ml and cultured for 24 h before harvesting for transfection. RAW/C4 cells (5×10^6 cells/transfection) were electroporated at 0.28 kV and 1000 microfarads using a Gene Pulser (Bio-Rad), whereupon they were centrifuged at 1000 rpm for 5 min and resuspended in 10 ml of culture medium and cultured at 37 °C. For stable transfection, 2 μg of selection plasmid (pNT-Neo, encoding geneticin resistance), 10 μg of expression plasmid (*Mitf*/pEF6), and 10 μg of reporter plasmid (pTRAP-eGFP) were used per transfection. After a 24-h recovery period,

transfected cells were cultured in selection media containing 450 μg/ml geneticin for 2 weeks. Colonies resistant to the antibiotic were pooled and expanded, and expression was monitored using a combination of Western blotting, flow cytometry analysis, and immunofluorescence. The cell lines generated were RAW/C4-GFP-pEF6 (empty expression vector) and RAW/C4-GFP-pEF6-*Mitf*-A (*Mitf* isoform-A expression vector).

Flow Cytometry Analysis of Fluorescently Activated Cells—Cells were washed with cold phosphate-buffered saline (PBS), centrifuged at 1000 rpm for 5 min, and resuspended in 0.5 ml of PBS for analysis of green fluorescent protein expression on a FACSCalibur flow cytometer (BD Biosciences). Data analysis was performed by analyzing 10,000 events for each assay using the Cellquest software package (BD Biosciences). The fluorescence intensity was divided into four regions, M1 to M4. M1 was set to encompass the background level of green autofluorescence exhibited by 99.9% of untransfected control cells; M2, M3, and M4 represented logarithmic increments of fluorescence intensity (100-, 1000-, and 10,000-fold above the background, respectively). All events with fluorescence intensity greater than the M1 region were accepted as cellular eGFP fluorescence events. The data are presented as shown in Equation 1,

$$\%\ \text{eGFP-expressing cells} = (M4)/(M2 + M3 + M4) \quad \text{(Eq. 1)}$$

Protein Isolation and Western Blotting—To isolate total cellular protein from cultured stable RAW/C4 cell lines, cells grown as monolayers were washed twice with PBS, pelleted, and then lysed with 500 μl of lysis buffer (66 mM Tris-HCl, pH 7.4, 2% SDS). Protein lysates were resolved by electrophoresis on a 0.1% SDS, 12% polyacrylamide gel, and blotted onto a nitrocellulose membrane (Immobilon transfer membrane; Millipore), which was blocked in 5% skim milk in Tris-buffered saline/Tween 20 (TBS-T) overnight at 4 °C. The V5 expressed protein tag encoded on the pEF6 vector was detected using a primary anti-V5 antibody (1:2000 dilution) (Serotec) by incubation for 2 h at room temperature. Membranes were washed and incubated with a secondary horseradish peroxidase-conjugated anti-mouse antibody (1:1000 dilution). Image development was performed using an enhanced chemiluminescent detection kit (Amersham Biosciences).

Immunofluorescence Detection of Exogenous Proteins—RAW/C4 stable cell lines grown on coverslips were washed twice with PBS and fixed with 4% paraformaldehyde in PBS. Cells were permeabilized with 0.1% Triton X-100 in PBS, and then the cells were washed in PBS containing 0.5% bovine serum albumin and labeled with primary anti-V5 antibody (1:2000 dilution) for 2 h. After washing with PBS, primary antibody was detected with a secondary goat anti-mouse phycoerythrin antibody (1:200 dilution) and incubated for 30 min. Cells were washed again with PBS and stained with DAPI (Sigma) for 15 min for visualization of nuclei. Cells were washed again and mounted onto glass coverslips using DAKO Cytomation fluorescent mounting media (Dako Corp., Carpenter, CA). Fluorescence microscopy was conducted on an Olympus AX-70 unit, and images were captured with NIH image 1.62 software using a Dage-MTI CCD300RC CCD camera.

Culturing OCLs in Vitro and Tartrate-resistant Acid Phosphatase Staining—For 5-day cultures, RAW/C4 cells were seeded at 3×10^4 cells in 10-cm tissue culture plastic plates (Corning Glass) and 5×10^3 cells/well in 6-well plates. For 7-day cultures, cells were seeded at 1×10^4 cells in 10-cm plates, 1.6×10^3 cells/well in 6-well plates, and 0.5×10^3 cells/well in 48-well plates. All wells were pre-coated with 0.1% gelatin (Sigma), and cells were grown in medium supplemented with 50 μg/ml ascorbic acid (Sigma), 40 ng/ml sRANKL, and 10^4 units/ml CSF-1 with medium changes every 2–3 days. OCL were observed after 5–7 days in culture. Cells were subsequently harvested and separately processed for total RNA extraction and for nuclear protein extraction. Alternatively, cells were fixed and stained for the OCL marker TRAP using a commercially available kit (387-A; Sigma) and scored as $TRAP^+$ multinucleated (more than three nuclei) cells.

Hematopoietic precursors were obtained from the spleens of wild type mice and the spleens of *mi/mi* mice. OCLs were grown in the presence of 80 ng/ml receptor activator of nuclear factor-κB (NF-κB) ligand (sRANKL, prepared as described (19)) and 200 units/ml colony-stimulating factor-1 (CSF-1) with medium changes every 3 days. Cells were harvested after 5 days in culture.

RNA Extraction and Quantitative PCR—Total cell RNA was extracted and purified from cells using the RNeasy mini-kit (Qiagen, Valencia, CA). Each sample was treated with DNase I (Ambion, Austin, TX) and reverse-transcribed using a 17-mer oligo(dT) primer and the Superscript III RNase H reverse transcriptase kit or Superscript III first-strand synthesis system for reverse transcription-PCR (Invitrogen) according to the manufacturer's instructions. Negative control samples (no first-strand synthesis) were prepared without the addition of reverse transcriptase. The cDNA was diluted to 100 μl with water, and 4 μl was used for quantitative real time PCR (qPCR) performed using the LightCycler-DNA Master SYBR Green I kit (Roche Applied Science). The PCR was performed using an ABI Prism thermal cycler (Applied Biosystems) as follows: 1 min hot start at 94 °C; 45 cycles of 15 s at 94 °C, 10 s at 60 °C, and 15 s at 72 °C. cDNA levels during the linear phase of amplification were normalized against *Hprt* (hypoxanthine phosphoribosyltransferase) controls. Assays were performed in triplicate, and the means ± S.D. were determined. Specific primers were used for qPCR as follows: mouse TRAP1C (GenBank™ accession number NM_007388) forward primer (5′-ACC TGT GCT TCC TCC AGG AT-3′) and reverse primer (5′-TCT CAG GGT GGG AGT GGG-3′); mouse cathepsin K (GenBank™ accession number NM_007802) forward primer (5′-CCA TAT GTG GGC CAG GAT G-3′) and reverse primer (5′-TCA GGG CTT TCT CGT TCC C-3′); mouse *Clcn7* (GenBank™ accession number NM_011930) forward primer (5′-GAC TGG CTG TGG GAA AGG AA-3′) and reverse primer (5′-TCT CGC TTG AGT GAT GTT GAC C-3′); mouse *Ostm1* (GenBank™ accession number NM_172416) forward primer (5′-TTG GAC AAT TAG TTC TAT CAT CG-3′) and reverse primer (5′-GCC GGA CTG TAA CAG ATA GCT-3′). The relative expression

levels were calculated using experimentally determined primer efficiency and the ΔC_T method (47).

Microarray Analysis and Data Handling—The microarray experiment was performed using 17.5 days post-coitum C57Bl/6J embryo total RNA as a common reference (48). Microarray experiments were performed in duplicate using independently generated RNA from OCL generated from the stable cell lines treated with sRANKL/CSF-1 for 5 days and untreated stable cell lines. The RNA was directly labeled during cDNA synthesis with amino allyl-conjugated Cy3 (sample) or Cy5 (embryo), as described on line, and hybridized at 42 °C overnight to 22,000 element mouse Compugen oligonucleotide microarrays (SRC, Microarray Facility). Slides were washed for 5 min in 2× SSC, 0.2% SDS buffer and scanned on a ScanArray 5000 confocal laser scanner. MolecularWare software (Digital Genome) was used to process the image, and data were corrected for local background, and confidence status was flagged for empty spots, signal/noise ratio, spot ratio variability, and spot morphology. Data were imported into the GeneSpring 4.2 software (Silicon Genetics) for clustering and comparative analysis.

Bioinformatic Extraction of 5′ Upstream Sequences of Compugen Array Gene List and Blast Analysis for Consensus MITF-binding Sites—The hypothetical promoters (2 kb upstream of the translation start site as defined in Ensembl) of all the genes on the 22,000 element Compugen array were extracted into a sequence-formatted file. String matching was employed to parse each promoter for the presence of M-box (TCANNTGA) motifs. This process entailed a 5′ to 3′ progression for each promoter sequence, with each position n receiving a score based on the agreement between each motif position i and the corresponding promoter sequence position $n + i$, where $i = 0.7$. For each motif position i, a match was worth 1, and a mismatch was worth 0. If the total score for the promoter sequence position n was equal to 8, a positive match was recorded for that position.

Analysis of Promoter Activity—RAW/C4 cells (5×10^6) were transfected with endotoxin-free plasmid preparations (Qiagen) by electroporation. Cells were electroporated (280 V/1 millifarads; Gene-Pulser, Bio-Rad) with 10 μg of reporter plasmid and 2 μg of expression plasmid in 250 μl of complete media supplemented with 10 mM HEPES (Thermotrace, San Diego). Cells were electroporated immediately after the addition of plasmid DNA and washed without delay after transfection to limit RAW264.7 activation by the plasmid DNA (49). After electroporation, the cells were divided into 2 or 4 wells of a 6-well tissue culture plate (Iwaki, Japan) and were cultured for 24 h before harvesting the cells. The cellular harvest and luciferase activity assay were performed using the Luclite luminescence reporter gene assay system (PerkinElmer Life Sciences) according to the manufacturer's instructions. Briefly, transfected cells were washed twice with cold PBS and extracted in the plate with 150 μl of 1× lysis buffer for 15 min. Cellular debris was removed by centrifugation, whereupon 50 μl of lysate supernatant was transferred into alternate wells of a 96-well Trilux Optiplate and assayed for luciferase activity by the addition of 50 μl of luciferase assay reagent. Light emission was measured with a Packard TriLux luminometer using Microbeta workstation software. Luciferase activity was normalized to the total protein concentration of the cell lysate as measured by the BCA assay kit (Pierce) to give relative light units per μg of protein. The mean ± S.E. was calculated within and between experiments.

Electrophoretic Mobility Gel Shift Assays (EMSA)—Nuclear extracts for EMSAs were prepared by hypotonic lysis at 4 °C. All buffers contained phosphatase inhibitors (1 mM sodium vanadate, 1 mM sodium pyrophosphate, 1 mM sodium molybdate, and 10 mM sodium fluoride) and a 1× protease inhibitor mixture (complete, mini, EDTA-free; Roche Applied Science) in all steps of nuclear extract preparation. Cells were harvested and washed twice in PBS. The pellet was resuspended in 1 ml per 10×10^6 cells of buffer A (10 mM HEPES, pH 7.6, 10 mM NaCl, 0.5 mM EDTA, 0.5 mM EGTA, 0.5 mM DTT, 0.5 mM PMSF). Cellular swelling was observed using phase-contrast microscopy. 0.5 ml per 10×10^6 cells of buffer B (25 mM HEPES, pH 7.6, 150 mM NaCl, 1 mM EDTA, 1 mM EGTA, 0.6% Nonidet P-40, 2 mM DTT, 1 mM PMSF) was added, and the solution was immediately vortexed at low speed for 30 s. Nuclei, free of cytoplasm, were apparent using light microscopy. The nuclei were pelleted, and the supernatant was removed completely. The nuclei were resuspended by addition of 100 μl of buffer C per 1×10^6 cells (25 mM HEPES, pH 7.6, 350 mM NaCl, 1 mM EDTA, 1 mM EGTA, 20% glycerol, 1 mM DTT, 0.5 mM PMSF) dropwise while flicking the tube. Nuclei were shaken vigorously in the high salt buffer for 20 min. Cellular debris was removed by centrifugation.

Complementary oligonucleotides used for double-stranded probe preparation were as follows with mutated residues shown in lowercase: (sense strand) TRAP from −582 to −549 relative to the ATG (5′-CAG TTC TGG GGA AGT CCA GTG CTC ACA TGA CCC A-3′) and TRAPΔE (5′-CAG TTC TGG GGA AGT CCA GTG CTc tcg agA CCC A-3′); *Clcn7* oligo 1 (5′-CGT GCA GCC ATA TGA AAT TTT ATT GT-3′) and *Clcn7* oligo 1ΔE (5′-CGT GCA GCc tcg agA AAT TTT ATT GT-3′); *Clcn7* oligo 2 (5′-CAC AGG AAA CAC ATG AAG CCA ACT TA-3′) and *Clcn7* oligo 2ΔE (5′-CAC AGG AAA ctc gag AAG CCA ACT TA-3′); *Clcn7* oligo 3 (5′-CGT CGT CAG TCA CGT GGG CAC CGA TG-3′) and *Clcn7* oligo 3ΔE (5′-CGT CGT CAG Tct cga gGG CAC CGA TG-3′); *Clcn7* oligo 4 (5′-CCG ATG ATA GAT CAC GTG AGA CCT GGG-3′) and *Clcn7* oligo 4ΔE (5′-CCG ATG ATA GAT ctc gag AGA CCT GGG-3′); and *Ostm1* oligo (5′-CAG TTC TGG GGA AGT CCA GTG CTC ACA TGA CCC A-3′) and *Ostm1*ΔE (5′-CAG TTC TGG GGA AGT CCA GTG CTc tcg agA CCC A-3′).

Oligonucleotides were 5′ end-labeled with [γ-^{32}P]ATP and T4 polynucleotide kinase for 30 min at 37 °C. Nuclear extract proteins were bound to the DNA probe in a 10-μl reaction containing 20 mM HEPES, pH 7.9, 500 nM DTT, 2 mM EDTA, 40 mM KCl, 12% glycerol, 1 μg of salmon sperm DNA, 0.04 pmol of purified probe, and 2 μg of nuclear extract. Reactions in which competitor probes were added included 10-, 50-, or 100-fold molar excess of unlabeled competitor probe (0.4, 2, or 4 pmol, respectively). The supershift reaction included the anti-MITF antibody (NeoMarkers). The Tris-glycine/EDTA gel system was used for EMSA analysis; 6% acrylamide/bisacrylamide gels

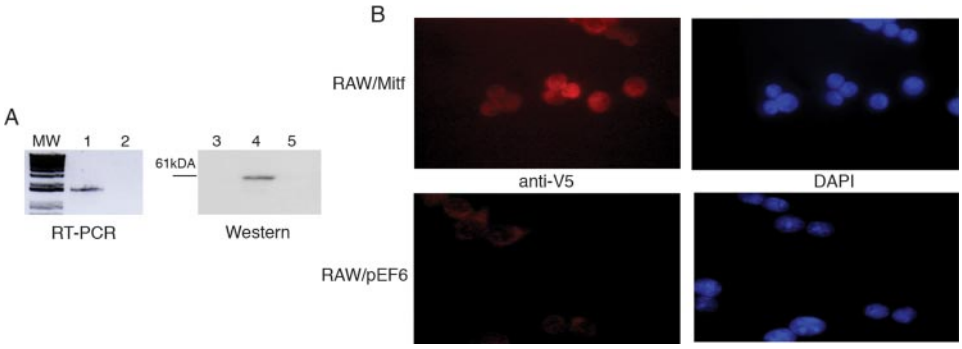

FIGURE 1. **Expression of MITF-*V5* in RAW264.7/C4 cells (RAW/C4 cells).** *A,* reverse transcription-PCR for *Mitf* transgene in stably transfected RAW/C4 cells using vector 5′ primer and *Mitf* reverse 3′ primer (*lane 1*). RNA from RAW/C4-pEF6 cell lines was used as a negative control (*lane 2*). Anti-V5 Western blot of total cell lysates from stably transfected RAW/C4 cells demonstrating MITF protein construct expression (*lane 4*). Cell lysates were resolved by SDS-PAGE and probed with anti-V5. Cell lysates from untransfected RAW/C4 cells and RAW/C4-pEF6 cells served as negative controls (*lanes 3* and *5,* respectively). *B,* detection of V5 epitope tagged MITF construct by immunofluorescence in stably transfected RAW/C4 cells using anti-V5 and phycoerythrin (*PE*)-conjugated anti-mouse antibodies. DAPI nuclear counter staining confirms MITF nuclear localization. The V5 epitope was undetectable in the RAW/pEF6 cell line.

(29:1) were polymerized by the addition of 0.1% w/v ammonium persulfate and 0.2% TEMED in 0.15 M Tris-HCl, pH 8.8.

Chromatin Immunoprecipitation (ChIP) Assay—To cross-link proteins to genomic DNA at indicated time points, formaldehyde was added to a final concentration of 1% to 2×10^6 bone marrow-derived cells treated with 40 ng/ml sRANKL, 1×10^4 units/ml CSF-1 and incubated at 37 °C for 10 min. The reaction was stopped by the addition of 125 mM glycine. The nuclei were isolated by resuspension in PIPES nuclei isolation buffer (5 mM PIPES, pH 8.0, 85 mM KCl, 0.5% Nonidet P-40, 1 μg/ml antipain, 1 μg/ml aprotinin, 1 μg/ml leupeptin, 1 mM PMSF, and phosphatase inhibitors where appropriate) by incubation on ice for 10 min and pelleting down at $500 \times g$ for 5 min at 4 °C. Soluble chromatin of an average size of 200–1000 bp was prepared using 30 cycles of 10-s pulses followed by a 20-s pause in a Branson 250 sonicator with a tapered microtip at 45% power. The chromatin was first precleared with protein G beads (Invitrogen) equilibrated with bovine serum albumin and yeast tRNA, and 10% of the soluble chromatin was set aside as input, and the rest of chromatin was immunoprecipitated with 5 μg each of anti-MITF or anti-PU.1 antibody. The immunoprecipitated DNA-protein complex was washed, eluted, decross-linked, treated with RNase A and proteinase K, and purified by Qiagen PCR purification kit according to the manufacturer's instructions.

RESULTS

Exogenous MITF Is Expressed in Stably Transfected RAW/C4 Cell Lines—To increase MITF expression in OCLs, a subclone of the osteoclastogenic RAW264.7 cell line (RAW/C4) was stably transfected to overexpress wild type MITF. RAW/C4 cells have an increased potential to form OCLs compared with the parent RAW264.7 cell line (45). MITF was cloned with a 3′ V5 epitope tag in the pEF6 mammalian expression plasmid, under the control of the EF1α promoter (50). The pEF6 and MITF/pEF6 plasmids were transfected separately into RAW/C4 cells together with the TRAP promoter reporter plasmid (pTRAP-eGFP) and pNT-Neo. Stable transfectants were selected using G418 and the resulting cell lines, RAW/C4-GFP-pEF6 and RAW/C4-GFP-*Mitf*/pEF6, were maintained as pools of clones rather than isolated clones to obviate insertion positional effects.

Expression of the pEF6-derived *Mitf*-V5 mRNA was detected by reverse transcription-PCR in the RAW/C4-GFP-*Mitf*/pEF6 cell line alone (Fig. 1*A*). Western blotting of native extracts of these cell lines using an anti-V5 antibody detected a 61-kDa protein, which was consistent with the size predicted for *Mitf*-V5 (Fig. 1*A*). Immunocytochemical staining of RAW/C4-GFP-*Mitf*/pEF6 and RAW/C4-GFP-pEF6 cells using anti-V5 antibody confirmed that exogenous V5-tagged MITF is expressed, and its intracellular localization to the nucleus was confirmed by DAPI nuclear counter staining (Fig. 1*B*).

Overexpression of MITF Increases OCL Number and Increases Expression of Known MITF Target Genes—The phenotypic outcome of MITF overexpression was determined when RAW/C4-GFP-*Mitf*/pEF6 cells were induced to form OCL by treatment with sRANKL and CSF-1. RAW/C4-GFP-*Mitf*/pEF6 cells formed OCLs that were larger and more strongly TRAP-positive than RAW/C4-GFP-pEF6 cell-derived OCLs (Fig. 2*A*). In a quantitative measurement of TRAP-positive, multinucleated cell formation (≥3 nuclei/cell), RAW/C4-GFP-*Mitf*/pEF6 cells were found to have a slightly greater potential to form OCLs than RAW/C4-GFP-pEF6 cells (Fig. 2*B*).

All cell lines were cotransfected with a murine TRAP promoter-eGFP reporter construct (pTRAP-eGFP) as an internal validated target of MITF activity. This construct incorporated a 620-bp fragment of the proximal murine TRAP 1C promoter that has been shown previously to be MITF-responsive (46), and flow cytometry was used to detect eGFP fluorescence. Fluorescence of eGFP was undetectable in the RAW/C4-GFP-pEF6 and RAW/C4 cell lines, whereas fluorescence was detected in the RAW/C4-GFP-*Mitf*/pEF6 cell line when examined with an Olympus IX-70 microscope using a fluorescein isothiocyanate filter (Fig. 2*C*). Flow cytometry was used to quantitate eGFP expression levels and determined that cells overexpressing MITF had a 2.5-fold increase in eGFP expression compared with the RAW/C4-GFP-pEF6 and RAW/C4-GFP cell lines (Fig. 2*D*).

Having confirmed that MITF overexpression in RAW/C4 cells is capable of regulating the expression of an exogenous TRAP promoter construct, we then examined the effect of MITF overexpression on the levels of endogenous genes. TRAP and cathepsin K mRNA levels were measured by qPCR before and after treatment of the cells with sRANKL and CSF-1 for 5 days.

The expression of endogenous TRAP in RAW/C4-GFP-*Mitf*/pEF6 cells on a macrophage background in the absence of

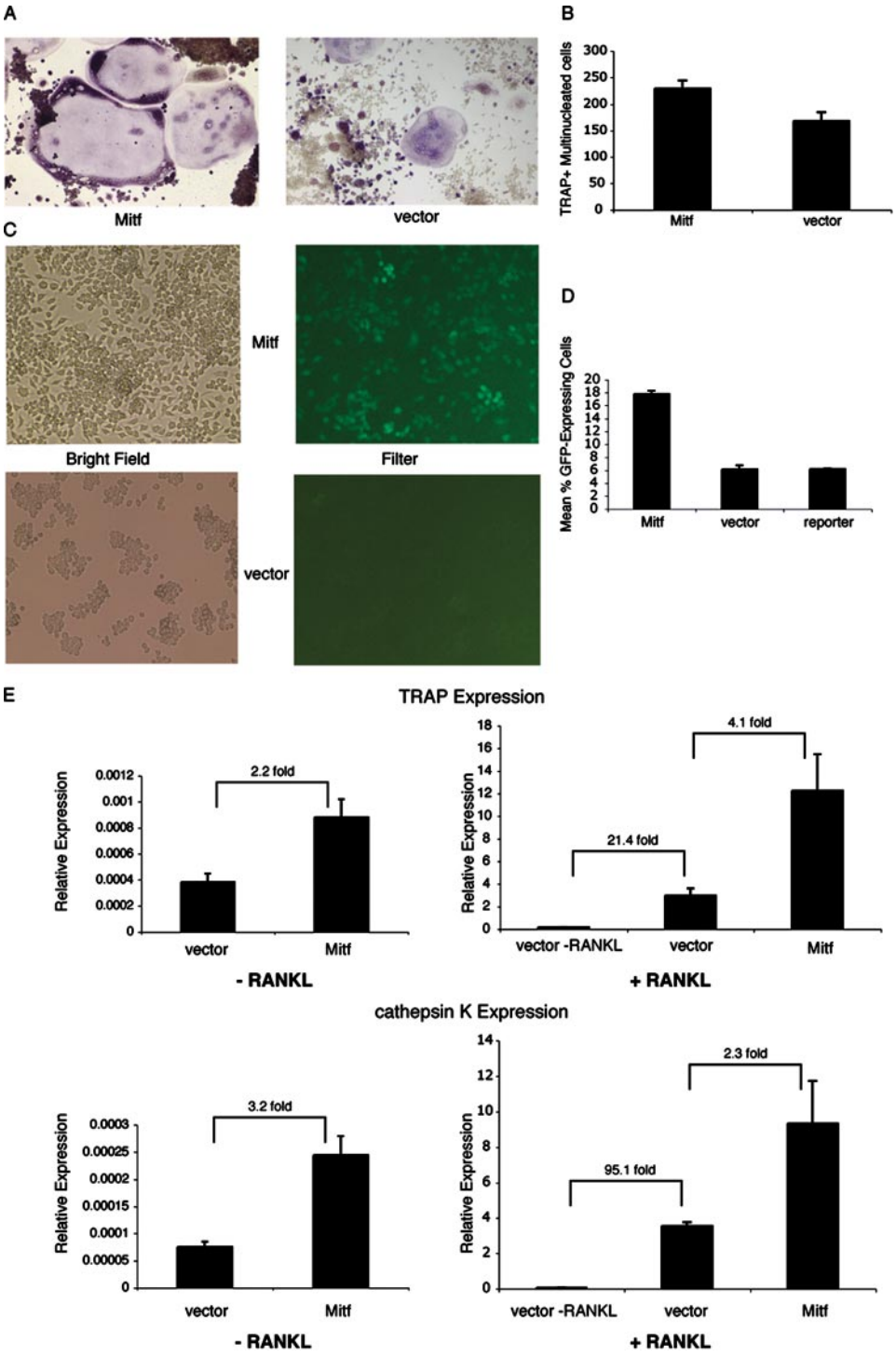

FIGURE 2. **Overexpression of MITF up-regulates osteoclast formation and increases the expression of known MITF targets TRAP and cathepsin K.** *A,* multinucleated OCLs derived from RAW/C4 cell stably transfected with MITF and empty vector (pEF6). *B,* quantitation of TRAP-positive multinucleated cells (>3 nuclei) following culture for with sRANKL/CSF-1. *Bars* represent means ± S.E. ($n = 9$). *C,* eGFP expression in stably transfected RAW/C4 cells using a TRAP promoter-eGFP reporter construct. Images were visualized on an Olympus IX-70 microscope using a fluorescein isothiocyanate filter and fluorescence specific to those cells expressing exogenous MITF. *D,* flow cytometry has been used to quantitate eGFP expression in stably transfected cells overexpressing MITF and TRAP promoter eGFP-reporter constructs. *Bars* represent means ± S.E. ($n = 9$). *E,* cells overexpressing MITF have a 2–3-fold increase in endogenous expression of both genes on a macrophage background (−*sRANKL*) compared with the vector control. TRAP and cathepsin K expression is increased (21.4- and 95.1-fold, respectively) following 5-day culture with sRANKL and CSF-1 in RAW/C4 cells (+*sRANKL*). Cells overexpressing MITF showed an increase in both TRAP and cathepsin K expression 2–4-fold higher than vector control cells ("superinduction") under the same conditions. Experiments were performed in triplicate, and the bars represent the S.D. for one experiment.

RANKL was 2.2-fold higher than in cells not overexpressing MITF, whereas cathepsin K was 3.2-fold higher (Fig. 2*E*). Following treatment of the vector control with sRANKL and CSF-1, endogenous TRAP expression was induced 21.4-fold, whereas cathepsin K expression was induced 95.1-fold. In the RAW/C4-GFP-*Mitf*/pEF6 cells following sRANKL and CSF-1 treatment, TRAP expression was superinduced a further 4.1-fold higher, whereas cathepsin K expression was superinduced 2.3-fold.

The superinduction of these genes in the RAW/C4-GFP-*Mitf*/pEF6 cell line suggests that a similar superinduction may occur with other MITF target genes. This suggests that increasing the level of MITF protein can result in a secondary increase in the level of activated phospho-MITF, which in turn can have a downstream effect on its transcriptional targets that can then be monitored using expression-profiling techniques.

Microarray and Bioinformatic Analysis of Genes Superinduced by MITF Overexpression during RAW/C4-derived Osteoclastogenesis—Phenotypic analysis of RAW/C4 cells in which the protein levels of MITF have been modulated has demonstrated that this is an effective cellular model to study MITF transcriptional targets. Microarray expression profiling of these cells was used to perform a global search for novel targets of MITF that are superinduced. RNA was harvested from RAW/C4-GFP-*Mitf*/pEF6 and RAW/C4-GFP-pEF6 cells on a macrophage background (untreated) or an OCL profile (5-day treatment with sRANKL and CSF-1) for this experiment. Labeled cDNA prepared from RAW/C4-GFP-*Mitf*/pEF6 and RAW/C4-GFP-pEF6 cells was hybridized to 22,000 element Compugen murine array chips, and the pattern of gene expression was analyzed.

In parallel to the microarray experiment, a bioinformatic analysis was undertaken to identify genes present on the Compugen array that

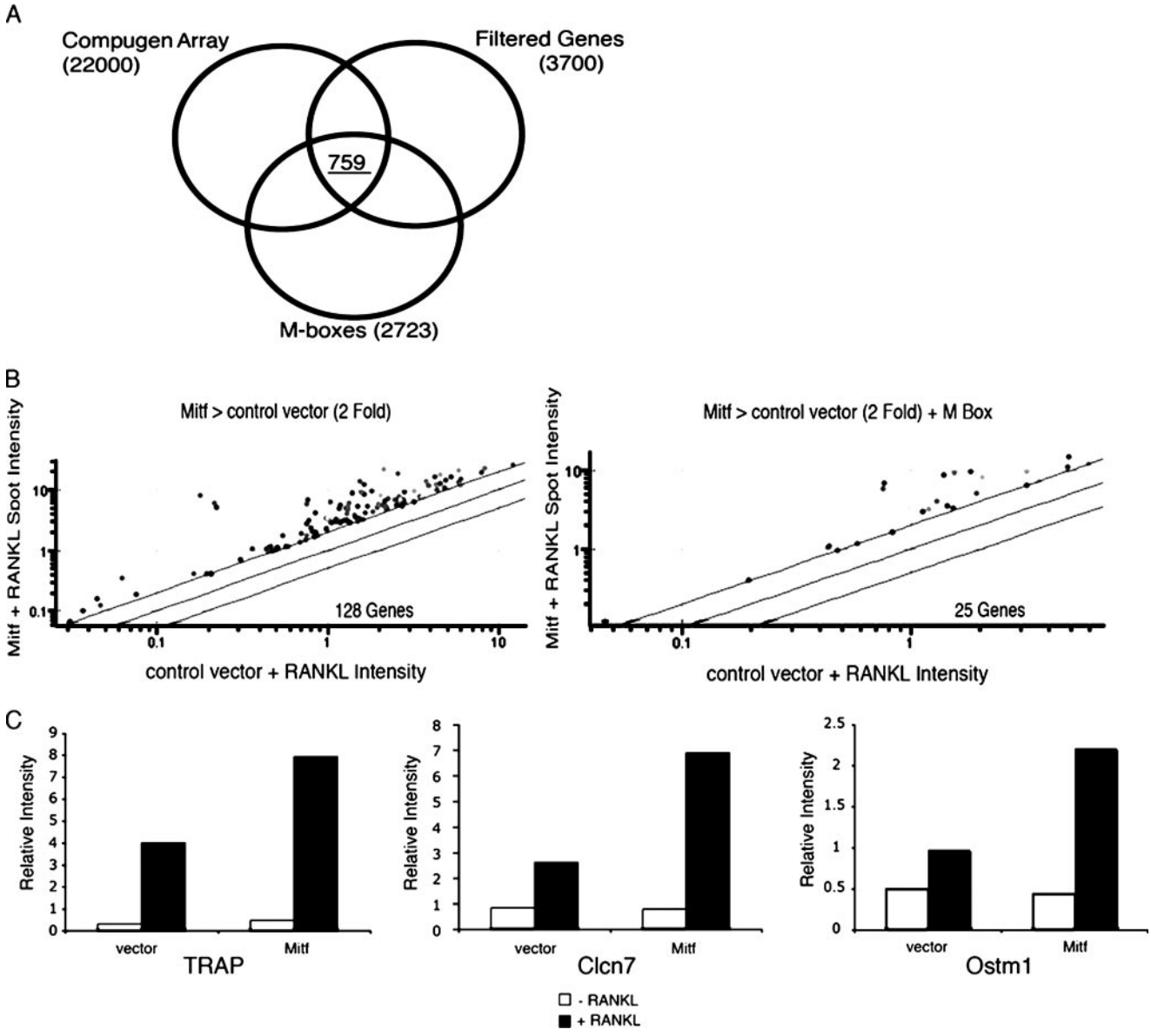

FIGURE 3. **Identification of genes superinduced by MITF overexpression during osteoclast differentiation in RAW/C4 cells.** Microarray analysis of analysis was performed using the murine Compugen 22,000 element array chips on RAW/C4, RAW/C4-pEF6, and RAW/C4-*Mitf*/pEF6 cell lines either untreated (0 days) or treated with 40 ng/ml sRANKL and 10^4 units/ml CSF-1 (5 days). In parallel, a bioinformatics analysis was undertaken to identify candidate M-box-containing genes. A large scale Blast technique has been developed to download 2 kb of DNA sequence 5′ of the translation start site for all the genes on the array. These promoter regions were searched for the presence of an extended *Mitf*-binding E-box consensus sequence (TCANNTGA), termed the M-box. *A,* Venn diagram compares the total genes on the array to the selected genes with high expression compared with embryo RNA (filtered genes) and to genes containing M-boxes. Common to all three groups is a list of 759 M-box containing genes with high expression on the array profile. *B,* data revealed a set of up-regulated genes following treatment with RANKL that were superinduced in cells overexpressing MITF. A list of 128 superinduced genes in MITF overexpressing cells was reduced to 25 on the basis of excluding genes without MITF-binding sites. *C,* expressions of TRAP, *Clcn7*, and *Ostm1* mRNAs are induced by sRANKL treatment of RAW/C4 cells for 5 days and superinduced by MITF overexpression. The microarray data were consistent with qPCR quantitation, and bioinformatics analysis identified *Clcn7* and *Ostm1* with a similar expression response. *Clcn7* and *Ostm1* are also induced by sRANKL treatment and are superinduced in cells overexpressing MITF.

contain consensus MITF-binding sites. A blast technique was undertaken to download 2 kb of genomic DNA sequence 5′ to the annotated translation start site for all genes represented on the Compugen array. These hypothetical promoter regions were searched for the presence of MITF-specific binding sites. MITF has been shown to bind to E-boxes (CANNTG) with affinity similar to other bHLH-ZIP transcription factors but with a preference for an additional T on the 5′ end or an A on the 3′ end (51). The bioinformatic approach utilized a blast algorithm to search for the sequence TCANNTGA (M-box; the additional defining nucleotides are underlined) in the hypothetical promoter regions of all the genes on the Compugen array.

The sample gene expression data were normalized against data from 17.5 days post-coitum embryo total RNA and filtered to remove uninformative spot data. The genes that passed filtering were analyzed for elevated expression relative to the embryo RNA, which produced a list of 3,700 genes. This gene list was compared with the gene list from the bioinformatic analysis of the Compugen gene regulatory regions containing candidate M-boxes (Fig. 3*A*). The working list of genes that was

TABLE 1
Genes superinduced by the overexpression of MITF during RAW/C4 osteoclastogenesis that contain candidate promoter M-boxes

Array identifier	GenBank™ accession no.	Gene name	Description
3003011_1	NM_008218	Hba1	Hemoglobin-α, adult chain 1
3002492_1	NM_007606	Car3	Carbonic anhydrase 3
3003286_1	NM_011930	Clcn7	Chloride channel 7
3002170_1	NM_007802	Ctsk	Cathepsin K
3002283_1	NM_008455	Kikb1	Kallikrein B, plasma 1
EXT_3106903_1	NM_013660	Sema4d	Sema domain, immunoglobulin domain (Ig)
3001911_1	NM_015774	Ero1l	ERO1-like (*S. cerevisiae*)
3006519_1	NM_011518	Syk	Spleen tyrosine kinase
3005446_1	NM_009856	Cd83	CD83 antigen
3004603_1	NM_013751	Hrasls	HRAS-like suppressor
3003846_1	NM_008357	Il15	Interleukin 15
EXT_3106319_1	NM_008830	Abcb4	ATP-binding cassette, subfamily B (MDR/TAP), member 4
3004290_1	NM_008445	Kif3c	Kinesin family member 3C
3003095_1	NM_010605	Kcnj5	Potassium inwardly-rectifying channel, subfamily J, member 5
3003615_1	NM_008185	Gstt1	Glutathione *S*-transferase, θ1
3003751_1	NM_009137	Ccl22	Chemokine (C-C motif) ligand 22
3002105_1	NM_008189	Guca1a	Guanylate cyclase activator 1a (retina)
EXT_3109859_1	AK004546	Ostm1	Osteopetrosis-associated transmembrane protein 1
3003836_1	NM_008620	Mpa2	Macrophage activation 2
3004515_1	NM_008679	TRAM1	Nuclear receptor coactivator 3
3002967_1	NM_020258	Slc37a2	Solute carrier family 37 (glycerol- 3-phosphate transporter), member 2
EXT_3111717_1	NM_022964	Wbscr5	Williams-Beuren syndrome chromosome region 5 homolog (human)
3005715_1	NM_013563	Il2rg	Interleukin 2 receptor, γ chain
3002705_1	NM_007388	Acp5	Acid phosphatase 5, tartrate-resistant

produced after excluding genes that did not meet these criteria was reduced from 22,000 gene expression profiles available for inspection on the array to a list of 759 expression profiles.

In addition to this filtering process, gene lists were sorted on a basis of fold-induction following treatment with sRANKL and CSF-1. Genes that were induced following treatment with sRANKL and CSF-1 were compared between two conditions, RAW/C4-GFP-*Mitf*/pEF6 (+sRANKL) and RAW/C4-GFP-pEF6 (+sRANKL) (Fig. 3*B*). Genes with transcript abundance at least 2-fold higher in the sRANKL-treated RAW/C4-GFP-*Mitf*/pEF6 cells compared with the RAW/C4-GFP-pEF6 cell line were selected for further analysis. This screen, based on fold-induction, produced a list of 128 genes that were "superinduced" by MITF expression in addition to sRANKL treatment. After excluding genes without M-boxes, this list was further reduced to 25 genes (Table 1). TRAP and cathepsin K were present in this short list of potential MITF-regulated genes, which are known osteoclast targets of MITF, and their presence validates this profiling approach. The microarray expression profiles of TRAP, *Clcn7*, and *Ostm1* display up-regulation of gene expression following culture with sRANKL and CSF-1 and further superinduction in cells overexpressing MITF (Fig. 3*C*). qPCR confirmed that *Clcn7* and *Ostm1* mRNA levels are induced following treatment with sRANKL and CSF-1 in RAW/C4-pEF6 cells and further induced in the RAW/C4-GFP-*Mitf*/pEF6 cell line (data not shown).

Time Course of Clcn7, Ostm1, and TRAP Expression and Identification of Promoter M-boxes—The up-regulation of TRAP, *Clcn7*, and *Ostm1* expression was examined in RAW/C4 cells over a 7-day time course of treatment with sRANKL and CSF-1. qPCR analysis of gene expression showed that both *Clcn7* (Fig. 4*B*) and *Ostm1* (*C*) were up-regulated with similar kinetics to TRAP (*A*), a known target of MITF.

A comparison of the mouse and human *Clcn7* promoter revealed four candidate M-boxes and numerous Ets transcription factor-binding sites (GGAA) located between −731 and +80 bp on both the forward and reverse strands of the proximal mouse promoter (Fig. 5*A*). Examination of the mouse *Ostm1* promoter revealed one candidate M-box, three E-boxes, and numerous Ets transcription factor-binding sites located between −534 and +70 on both the forward and reverse strands of the proximal promoter (Fig. 5*B*).

Clcn7 mRNA Levels Are Reduced in mi/mi Osteoclasts—*Clcn7* mRNA expression is induced by overexpression of MITF protein in RAW/C4 cells, but is *Clcn7* expression affected in OCLs derived from *mi/mi* mice? The *mi/mi* mouse has a dominant negative mutation in MITF such that it is able to bind to its dimerization partners without activating transcription of known targets like TRAP and cathepsin K, therefore rendering MITF, as well as its partners, functionally inactive.

TRAP and *Clcn7* mRNA levels were measured by qPCR in RNA preparations of cells from wild type and *mi/mi* spleens cultured with sRANKL and CSF-1. Expression of both TRAP and *Clcn7* increase over a period of 5 days in culture, consistent with genes that are induced during osteoclastogenesis (Fig. 6). In bone marrow-derived OCL differentiated *in vitro* from *mi/mi* mice, the induction of both TRAP and *Clcn7* is ablated, but the basal expression of *Clcn7* is not diminished.

MITF Binds to the Clcn7 Promoter—To establish whether MITF directly transcriptionally regulates *Clcn7* expression in osteoclasts, the ability of MITF to bind to the *Clcn7* promoter in primary and RAW/C4-derived OCLs was determined. Experiments validating the direct interaction of MITF with potential targets in a functional manner are well established in cell line models, including RAW264.7 cells (6, 7, 10, 19, 39, 46, 52).

ChIP assays for MITF and the Ets transcription factor, PU.1, which can act as a transcriptional coactivator with MITF, were performed on nuclear extracts from wild type bone marrow cells following treatment with sRANKL and CSF-1 in culture over a time course of 5 days. qPCR amplification of the region containing M-boxes on chromatin cross-linked to anti-MITF or anti-PU.1 antibodies revealed that both MITF and PU.1 were bound to the endogenous *Clcn7* promoter region with increased abundance over the 5-day time course (Fig. 7*A*). The

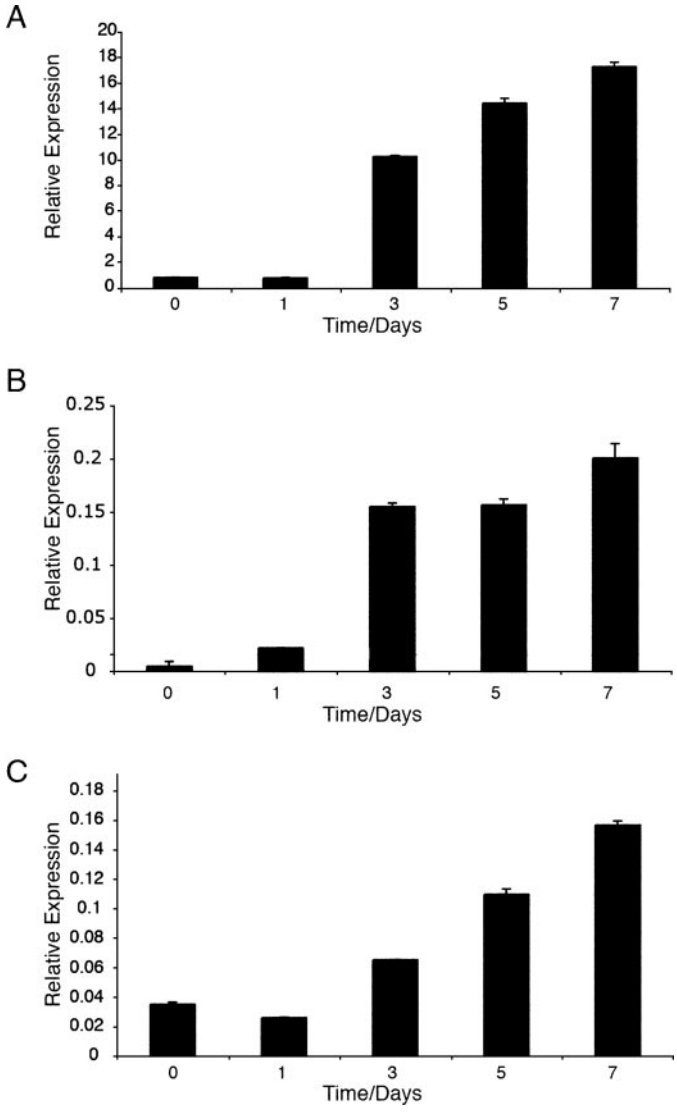

FIGURE 4. **TRAP, *Clcn7*, and *Ostm1* are up-regulated with similar kinetics during osteoclastogenesis.** qPCR for TRAP (*A*), *Clcn7* (*B*), and *Ostm1* (*C*) in RAW/C4 cells cultured with sRANKL and CSF-1 over a time course of 7 days. Expression of TRAP, *Clcn7*, and *Ostm1* was induced after 3 days reaching maximal expression between 5 and 7 days. All three genes display similar kinetics of expression during the time course. Experiments were performed in triplicate, and the *bars* represent the standard deviation for one experiment.

detection of MITF binding as well as the binding of its cotranscriptional activator, PU.1, on the *Clcn7* promoter supports the *in vitro* evidence that MITF directly regulates transcription of *Clcn7* in primary osteoclasts.

Radiolabeled oligonucleotide probes specific for the M-boxes identified in the *Clcn7* promoter were designed for EMSA. A probe from the region of the TRAP promoter previously shown to have specific MITF binding (6) was used to optimize conditions (Fig. 7*B*). Endogenous MITF from nuclear extracts of RAW/C4 cells cultured with sRANKL and CSF-1 for 5 days was found to bind specifically to probes 2, 3, and 4 as shown by the supershift that occurs in the presence of a mouse anti-MITF antibody (Fig. 7*C*). Binding specificity was demonstrated using cold competition assays performed with the wild type M-box oligonucleotides and mutated M-box oligonucleotides in which the CANNTG core was mutated to CTCGAG. Minor nonspecific bands were present in the EMSA for probe 1. Examination of the proximal promoters of the human, mouse, and rat *Clcn7* genes revealed that only M-boxes 3 and 4 are conserved between these species (Fig. 7*D*). The EMSAs identify specific sites of MITF binding (M-boxes 3 and 4) within the *Clcn7* promoter that are conserved between human, mouse, and rat.

MITF but Not mi Expression Constructs Transactivate the Clcn7 Promoter—Transient transfections of transcription factor expression plasmids were performed in RAW/C4 cells to assess the activity and responsiveness of the proximal *Clcn7* promoter. *Mitf, mi,* and empty vector expression constructs were cotransfected with a *Clcn7* promoter (−731 to +80) luciferase reporter construct. The *Clcn7* promoter was transactivated by the wild type *Mitf* expression construct but not by the *mi* (dominant negative) expression construct (Fig. 8). To determine which individual M-boxes are necessary for this transactivation, specific M-box mutant constructs were examined (Fig. 8). All of the four consensus M-boxes were mutated (M1–M4) in separate constructs. Mutations of M1, M2, or M3 had no effect on *Clcn7* transactivation by MITF, although mutation of M4, the site adjacent to the transcription start site, caused complete inhibition of luciferase expression in cells transiently transfected with wild type MITF. Interestingly, mutation of M3 reduced basal luciferase activity 2-fold, although this promoter construct was still responsive to transient increases in wild type MITF protein. A construct containing mutations of all four M-boxes (M1–M4) had reduced levels of basal luciferase activity and was not responsive to transient overexpression of wild type MITF protein. These data suggest that MITF transactivates the *Clcn7* promoter *in vitro* via M4. Basal expression of *Clcn7* involves M3 and unidentified factors but not MITF. These EMSA and cell transfection assays demonstrate a consistent ability of MITF to bind to and transactivate the Clcn7 promoter via at least one M-box.

MITF Binds and Transactivates the Ostm1 Promoter—EMSA was performed on oligonucleotide probes specific for the M-box identified in the *Ostm1* promoter. Endogenous MITF from nuclear extracts of RAW/C4 cells cultured with sRANKL and CSF-1 for 5 days bound specifically to the probe as shown by the supershift, which occurs in the presence of an anti-MITF antibody (Fig. 9*A*). Binding specificity was demonstrated using cold competition assays performed with a wild type M-box oligonucleotide and a mutated M-box oligonucleotide in which the CANNTG core was mutated to CTCGAG. These experiments thereby identified a specific MITF-binding site within the *Ostm1* promoter.

A 600-bp fragment of the murine *Ostm1* promoter (−534 to +63) was cloned into pGL2-Basic (p*Ostm1*-Luc). The responsiveness to MITF of p*Ostm1*-Luc was assayed by cotransfection of the plasmid into RAW/C4 cells with an *Mitf, mi,* or empty vector expression construct. The *Ostm1* promoter was transactivated by the wild type *Mitf* expression construct but not by the *mi* expression construct (Fig. 9*B*). This indicates that MITF can activate transcription of a 600-bp fragment of the *Ostm1* promoter and that this is likely to be mediated through MITF binding to the M-box identified within this region. The EMSA and

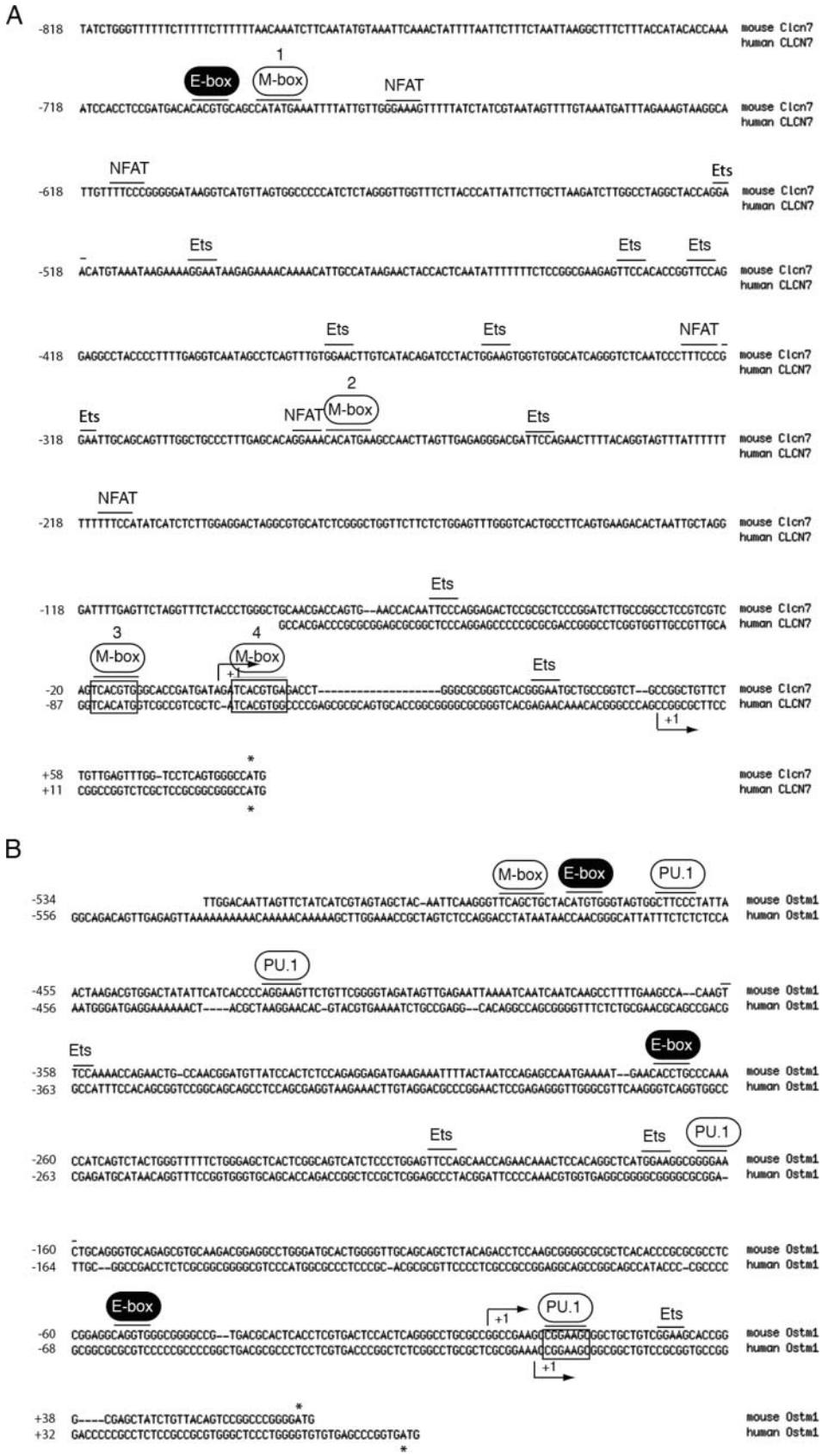

FIGURE 5. **ClustalW alignment of the mouse and human *Clcn7* and *Ostm1* promoter regions.** The conserved promoter regions between mouse and human have been aligned for the *Clcn7* and *Ostm1* genes. *A,* proximal promoter region of the *Clcn7* gene contains four potential M-boxes. The candidate M-boxes are labeled M-box 1–4. M-boxes 1–3 occur in the 5′ region upstream of the transcription start site, and M-box 4 is located in the 5′-untranslated region immediately adjacent to the transcription start site. *B,* candidate *Ostm1* M-box is labeled along with three other weak MITF-binding sites (E-boxes). *Arrows* indicate transcription start sites for mouse and human, and *asterisks* indicate the translation start sites. Conserved and aligned transcription factor-binding sites are *boxed.*

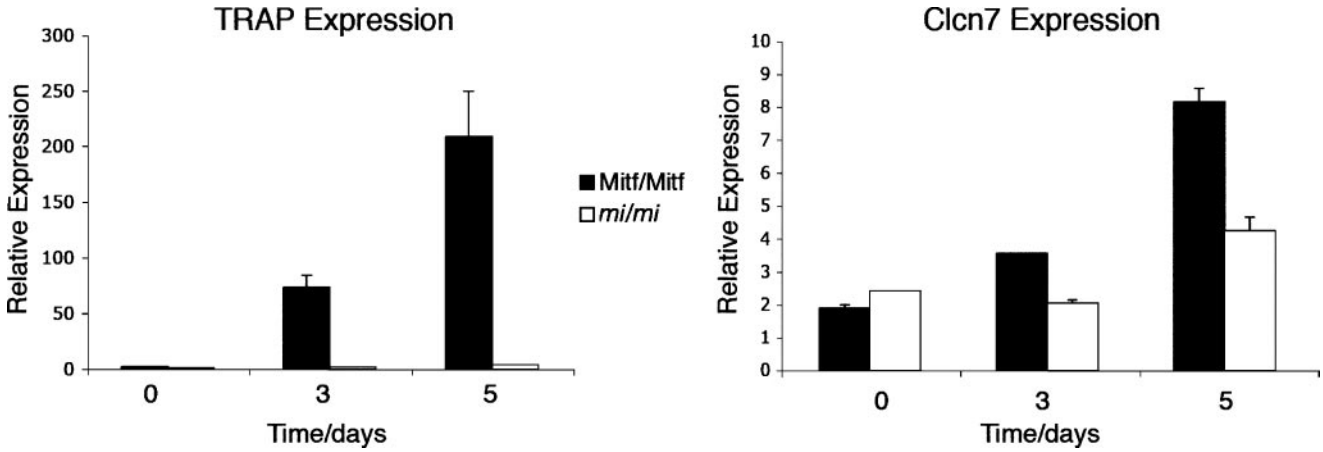

FIGURE 6. **qPCR analysis of TRAP and *Clcn7* mRNA levels.** Bone marrow-derived OCL from C57/BL6 and *mi/mi* mice on a C57/BL6 background over a 5-day culture with 40 ng/ml sRANKL and 10^4 units/ml CSF-1. Both TRAP and *Clcn7* expression levels increased over the 5-day time course in the wild type mice. The induction of both TRAP and *Clcn7* expression was ablated in the *mi/mi* mice. Experiments were performed in triplicate, and the *bars* represent the standard deviation for one experiment.

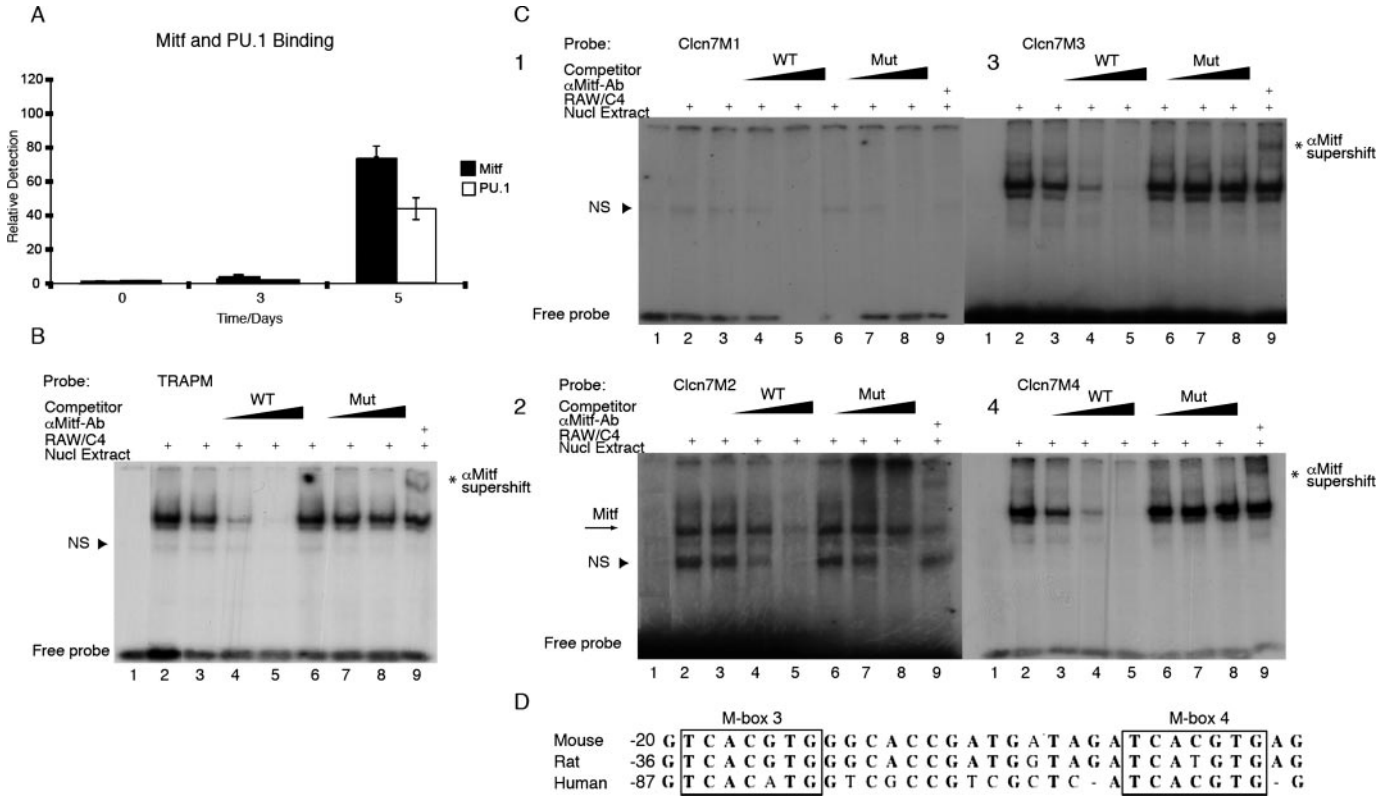

FIGURE 7. **ChIP and EMSA confirm MITF binding to specific regions within the *Clcn7* promoter.** *A,* nuclear extracts were prepared from C57/BL6 bone marrow cells following culture with 40 ng/ml sRANKL and 1×10^4 units/ml CSF-1 over a period of 0–5 days. Using anti-MITF and anti-PU.1 antibodies to isolate chromatin fragments, qPCR was able to detect an increase in abundance of the *Clcn7* promoter region bound to the respective proteins over the time course. Experiments were performed in triplicate, and the *bars* represent the S.D. for one experiment. *B,* nuclear extracts from RAW/C4 cells treated with sRANKL and CSF-1 (5 days) incubated with a probe from the TRAP promoter region to optimize EMSA conditions. *WT,* wild type; *Mut*, mutant; *Ab,* antibody; *NS*, not significant. *C,* the same nuclear extracts were incubated with probes containing the four M-boxes from the *Clcn7* promoter region. MITF binding specificity was demonstrated with cold competition with both wild type and E-box mutation oligonucleotides (*arrow*). Incubation with an anti-MITF antibody produces a supershifted band (*). Selective loss of the MITF complex by wild type and not mutant competitors suggests that MITF has specificity for M-box probes 2, 3, and 4. No specific complex was seen in probe 1. *D,* M-boxes 3 and 4 are conserved between human, mouse, and rat species.

cell transfection data indicate that MITF transcriptionally regulates the *Ostm1* proximal promoter.

DISCUSSION

The differentiation of myeloid progenitor cells into bone-resorbing osteoclasts depends upon lineage-specific extracellular signaling molecules, CSF-1, and RANKL. The binding of these factors to their respective cognate receptors, CSF-1R (c-Fms) and RANK, initiates changes in the pattern of transcriptional regulation that direct changes in both the phenotype and activity of pre-osteoclasts and osteoclasts. MITF is a member of the b-HLH-ZIP MiT subfamily of transcription fac-

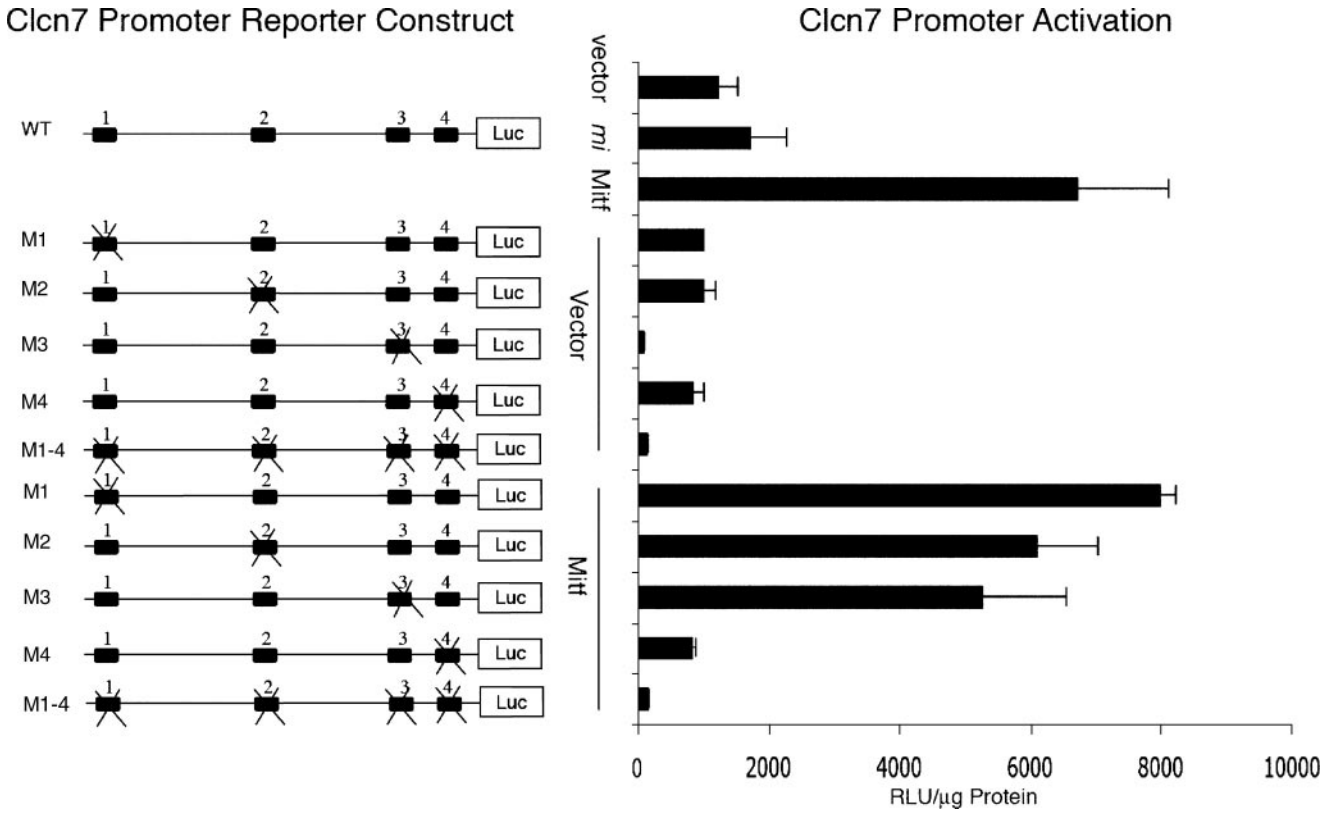

FIGURE 8. **Overexpression of wild type MITF protein, but not *mi*, transactivates *Clcn7* promoter reporter constructs via a specific M-box.** *Clcn7* promoter-luciferase constructs are graphically represented (*schematic*) beside their respective relative luciferase activities (*histogram*). The four M-boxes within the promoter have been mutated consecutively in separate constructs (*M1–M4*) and all together in one construct (*M1–4*). Vector refers to the empty expression construct pEF6. Overexpression of MITF protein transactivates the wild type (*WT*), *Clcn7*pM1 (*M1*), *Clcn7*pM2 (*M2*), and *Clcn7*pM3-Luc (*M3*) reporter constructs compared with basal levels. Basal levels (vector or *mi*) of luciferase reporter activity are reduced in transfection experiments with the *Clcn7*pM3- and *Clcn7*pM1–4-Luc (M1–4) reporter constructs. Cotransfections with MITF were unable to transactivate *Clcn7*pM4-Luc or *Clcn7*pM1–4-Luc constructs. *Bars* represent means ± S.E. ($n = 9$).

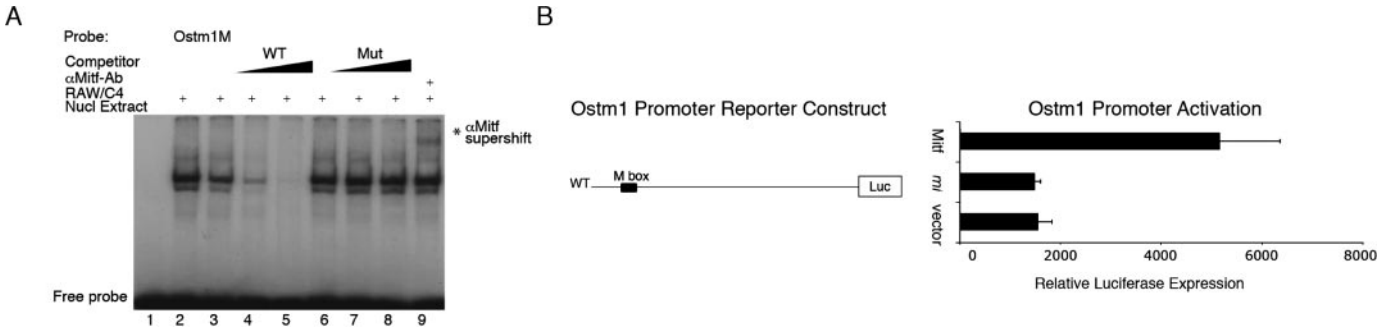

FIGURE 9. **EMSA confirmed MITF binding to an M-box containing probe within the *Ostm1* promoter region, and MITF transactivates the *Ostm1* promoter.** *A,* nuclear extracts from RAW/C4 cells treated with sRANKL and CSF-1 (5 days) incubated with probes containing the M-box from the *Ostm1* promoter region. MITF binding specificity was demonstrated with cold competition with both wild type (*WT*) and E-box mutation (*Mut*) oligonucleotides (*arrowhead*). Incubation with an anti-MITF antibody produces a supershifted band (*). Selective loss of the MITF complex by wild type and not mutant competitors suggests that MITF has specificity for the M-box probe. *Ab*, antibody. *B,* cotransfections with *Mitf*/pEF6 produce a 3-fold induction in relative luciferase (*Luc*) activity compared with basal levels and transfections with *mi*/pEF6. *Bars* represent means ± S.E. ($n = 9$).

tors that have been shown to regulate the process of gene expression in osteoclasts (16). MITF forms heterodimers with other MiT factors, TFE3, TFEB, and TFEC, to activate transcription of its target genes. Terminally differentiated osteoclasts express all members of the MiT family of factors, so any one of these factors is therefore capable of regulating gene expression in osteoclasts (10).

The genes transcriptionally activated by MITF, including TRAP (6, 19, 46) and cathepsin K (7), are late markers of osteoclastogenesis and have functional roles in bone resorption. The function of TRAP *in vivo* remains unclear, but it appears to regulate attachment of the osteoclast through dephosphorylation of $\alpha_v\beta_3$ integrin phosphoprotein ligands, including osteopontin and bone sialoprotein (53). TRAP participates in reactive oxygen species-mediated hydrolysis of collagen through the generation of ·OH radicals (54). Proteolytic nicking of human TRAP can activate it as an ATPase at neutral pH thereby potentially regulating the extracellular ATP concentration (55). On the other hand cathepsin K is the major cysteine protease that hydrolyzes the collagen matrix. When cathepsin

K is inactivated there is a profound loss of osteoclastic bone resorption activity in both cathepsin $K^{-/-}$ mice (56) and in the human disease, pycnodysostosis, where there are inactivating mutations in the cathepsin K gene (57, 58).

To identify the set of osteoclast-expressed genes that are regulated by MITF, we have taken the approach of overexpressing MITF in the RAW/C4 cell line. An alternative approach of expressing the dominant negative *mi* was considered, but we judged that the inactivation approach was likely to have more profound consequences for osteoclast function based on the biology of known MITF target genes as well as pleiotropic effects on gene expression, which would make interpretation more difficult. Expression of the *mi* dominant negative form of MITF in osteoclasts or in RAW/C4-derived OCL will inactivate wild type MITF in homodimers and TFE3, TFEB, and TFEC as heterodimers (9, 16). The effects of this dysregulation of the MiT family on transcriptional control of MITF/TFE target genes are likely to be more profound than that induced by elevation of the level of MITF alone. The increase in MITF through transient coexpression with promoter-reporter gene constructs results in an increase in promoter activity of MITF target genes in RAW264.7 macrophages and in the RAW/C4 subclone. Phosphorylation of MITF on Ser-307 by p38 MAP kinase in response to RANKL binding to RANK in osteoclasts is required for transactivation of TRAP gene expression (19). The gene induction observed with overexpression of MITF in RAW/C4 cells indicates that the level of MITF is limiting for target gene expression.

In this study, we have combined expression profiling with a bioinformatic search for the presence of M-boxes, and as a result we have identified a set of genes that are superinduced by MITF overexpression in RAW/C4 cells undergoing osteoclastogenesis and contain candidate M-boxes in their promoter regions. The regulation by MITF of two of these genes, the chloride channel *Clcn7* and the *Ostm1*, was examined in detail. Assays of functionality of the M-boxes by EMSA with nuclear extracts of RAW/C4 cells confirmed that sites within the promoters of *Clcn7* and *Ostm1* could bind MITF as determined by cold competition and supershifting with an anti-MITF antibody. The coordinate expression of these genes was examined over a time course of osteoclastogenesis, and they were induced with similar kinetics to each other and to TRAP.

CLCN7 is a chloride channel localized to late endosomes, lysosomes, and the ruffled border in osteoclasts, where it acts with the vacuolar H^+-ATPase to acidify the resorptive space. The loss or functional inactivation of CLCN7 causes osteopetrosis as well as neurodegeneration and a severe lysosomal storage disease (59). The G215R mutation in the human *CLCN7* gene is associated with autosomal dominant osteopetrosis type II, and patients are characterized by a loss of osteoclast function despite no significant changes in the standard parameters of osteoclast differentiation, phenotype, and the expression of osteoclast markers (60).

The phenotype of $Clcn7^{-/-}$ mice is strikingly similar to the mutant grey-lethal *gl/gl* mice that are characterized by retinal and central nervous system degeneration, pigmentation changes, and osteopetrosis. The *gl* mutation is a deletion resulting in complete loss of function of OSTM1 (61). The murine *gl* gene encodes a 338-amino acid type I transmembrane protein that localizes to the intracellular compartment. Mutation in the human *GL* (*OSTM1*) gene leads to severe recessive osteopetrosis. Characterization of an autosomal recessive malignant infantile osteopetrosis individual revealed a homozygous 2-bp deletion in exon 2 of *OSTM1* and is characterized by severe osteosclerosis, pathologic fractures, hepatosplenomegaly, and pancytopenia (43). Activity of the murine gl protein is absolutely required for osteoclast and melanocyte maturation and function (61).

Recently the analysis of OSTM1 association with CLCN7 demonstrated that OSTM1 requires CLCN7 to localize to lysosomes, whereas the formation of a CLCN7-OSTM1 complex is required to stabilize CLCN7 (44). In osteoclasts, OSTM1 and CLCN7 colocalize with the a3 subunit of the V-type H^+-ATPase in the ruffled border (44). The loss of osteoclast function that occurs in the *gl* mutation with the loss of OSTM1 may therefore result from a secondary reduction in CLCN7 protein levels. *Clcn7* mRNA levels in *gl* mice are unchanged, and *Ostm1* mRNA levels are unchanged in $Clcn7^{-/-}$ mice, whereas the OSTM1 protein is undetectable in $Clcn7^{-/-}$ osteoclasts (44). In our studies the basal level of *Ostm1* was relatively high but was further induced by RANKL treatment, whereas the basal level of *Clcn7* was very low but it was highly inducible with RANKL treatment. Induction of *Clcn7* during osteoclastogenesis may induce association of a pre-existing pool of OSTM1 and translocate to the lysozyme and from there to the ruffled border.

In summary, we have used a cell line model of osteoclastogenesis in which we have increased the amount of MITF. The superinduction of gene expression associated with both osteoclastogenesis and MITF overexpression was identified by microarray analysis, and the list of candidate MITF target genes was refined by bioinformatic analysis of the gene promoters for candidate M-boxes. We identified the critical osteoclast functional genes *Clcn7* and *Ostm1* as MITF targets and characterized the regulation by MITF of these genes.

REFERENCES

1. Tondravi, M. M., McKercher, S. R., Anderson, K., Erdmann, J. M., Quiroz, M., Maki, R., and Teitelbaum, S. L. (1997) *Nature* **386,** 81–84
2. Wang, Z. Q., Ovitt, C., Grigoriadis, A. E., Steinlein, U. M., Ruther, U., and Wagner, E. F. (1992) *Nature* **360,** 741–745
3. Franzoso, G., Carlson, L., Xing, L., Poljak, L., Shores, E. W., Brown, K. D., Leonardi, A., Tran, T., Boyce, B. F., and Siebenlist, U. (1997) *Genes Dev.* **11,** 3482–3496
4. Iotsova, V., Caamano, J., Loy, J., Yang, Y., Lewin, A., and Bravo, R. (1997) *Nat. Med.* **3,** 1285–1289
5. Xing, L., Bushnell, T. P., Carlson, L., Tai, Z., Tondravi, M., Siebenlist, U., Young, F., and Boyce, B. F. (2002) *J. Bone Miner. Res.* **17,** 1200–1210
6. Luchin, A., Purdom, G., Murphy, K., Clark, M. Y., Angel, N., Cassady, A. I., Hume, D. A., and Ostrowski, M. C. (2000) *J. Bone Miner. Res.* **15,** 451–460
7. Motyckova, G., Weilbaecher, K. N., Horstmann, M., Rieman, D. J., Fisher, D. Z., and Fisher, D. E. (2001) *Proc. Natl. Acad. Sci. U. S. A.* **98,** 5798–5803
8. Moore, K. J. (1995) *Trends Genet.* **11,** 442–448
9. Hemesath, T. J., Steingrímsson, E., McGill, G., Hansen, M. J., Vaught, J., Hodgkinson, C. A., Arnheiter, H., Copeland, N. G., Jenkins, N. A., and Fisher, D. E. (1994) *Genes Dev.* **8,** 2770–2780
10. Rehli, M., Lichanska, A., Cassady, A. I., Ostrowski, M. C., and Hume, D. A. (1999) *J. Immunol.* **162,** 1559–1565

11. Tassabehji, M., Newton, V. E., and Read, A. P. (1994) *Nat. Genet.* **8,** 251–255
12. Amiel, J., Watkin, P. M., Tassabehji, M., Read, A. P., and Winter, R. M. (1998) *Clin. Dysmorphol.* **7,** 17–20
13. Nomura, S., Sakuma, T., Higashibata, Y., Oboki, K., and Sato, M. (2001) *J. Bone Miner. Metab.* **19,** 183–187
14. Graves, L., III, and Jilka, R. L. (1990) *J. Cell. Physiol.* **145,** 102–109
15. Glowacki, J., Cox, K. A., and Wilcon, S. (1989) *Bone Miner.* **5,** 271–278
16. Steingrímsson, E., Copeland, N. G., and Jenkins, N. A. (2004) *Annu. Rev. Genet* **38,** 365–411
17. Hemesath, T. J., Price, E. R., Takemoto, C., Badalian, T., and Fisher, D. E. (1998) *Nature* **391,** 298–301
18. Wu, M., Hemesath, T. J., Takemoto, C. M., Horstmann, M. A., Wells, A. G., Price, E. R., Fisher, D. Z., and Fisher, D. E. (2000) *Genes Dev.* **14,** 301–312
19. Mansky, K. C., Sankar, U., Han, J., and Ostrowski, M. C. (2002) *J. Biol. Chem.* **277,** 11077–11083
20. Ferguson, C. A., and Kidson, S. H. (1997) *Pigm. Cell Res.* **10,** 127–138
21. Adachi, S., Morii, E., Kim, D., Ogihara, H., Jippo, T., Ito, A., Lee, Y. M., and Kitamura, Y. (2000) *J. Immunol.* **164,** 855–860
22. Carreira, S., Liu, B., and Goding, C. R. (2000) *J. Biol. Chem.* **275,** 21920–21927
23. Turque, N., Denhez, F., Martin, P., Planque, N., Bailly, M., Begue, A., Stehelin, D., and Saule, S. (1996) *EMBO J.* **15,** 3338–3350
24. Baxter, L. L., and Pavan, W. J. (2003) *Gene Expr. Patterns* **3,** 703–707
25. Du, J., Miller, A. J., Widlund, H. R., Horstmann, M. A., Ramaswamy, S., and Fisher, D. E. (2003) *Am. J. Pathol.* **163,** 333–343
26. McGill, G. G., Horstmann, M., Widlund, H. R., Du, J., Motyckova, G., Nishimura, E. K., Lin, Y. L., Ramaswamy, S., Avery, W., Ding, H. F., Jordan, S. A., Jackson, I. J., Korsmeyer, S. J., Golub, T. R., and Fisher, D. E. (2002) *Cell* **109,** 707–718
27. Ge, Y., Jippo, T., Lee, Y. M., Adachi, S., and Kitamura, Y. (2001) *Am. J. Pathol.* **158,** 281–292
28. Jippo, T., Lee, Y. M., Katsu, Y., Tsujino, K., Morii, E., Kim, D. K., Kim, H. M., and Kitamura, Y. (1999) *Blood* **93,** 1942–1950
29. Morii, E., Jippo, T., Tsujimura, T., Hashimoto, K., Kim, D. K., Lee, Y. M., Ogihara, H., Tsujino, K., Kim, H. M., and Kitamura, Y. (1997) *Blood* **90,** 3057–3066
30. Morii, E., Tsujimura, T., Jippo, T., Hashimoto, K., Takebayashi, K., Tsujino, K., Nomura, S., Yamamoto, M., and Kitamura, Y. (1996) *Blood* **88,** 2488–2494
31. Murakami, M., Ikeda, T., Ogawa, K., and Funaba, M. (2003) *Biochem. Biophys. Res. Commun.* **311,** 4–10
32. Ito, A., Morii, E., Maeyama, K., Jippo, T., Kim, D. K., Lee, Y. M., Ogihara, H., Hashimoto, K., Kitamura, Y., and Nojima, H. (1998) *Blood* **91,** 3210–3221
33. Tsujimura, T., Morii, E., Nozaki, M., Hashimoto, K., Moriyama, Y., Takebayashi, K., Kondo, T., Kanakura, Y., and Kitamura, Y. (1996) *Blood* **88,** 1225–1233
34. Jippo, T., Morii, E., Tsujino, K., Tsujimura, T., Lee, Y. M., Kim, D. K., Matsuda, H., Kim, H. M., and Kitamura, Y. (1997) *Blood* **90,** 2601–2608
35. Ito, A., Jippo, T., Wakayama, T., Morii, E., Koma, Y., Onda, H., Nojima, H., Iseki, S., and Kitamura, Y. (2003) *Blood* **101,** 2601–2608
36. Morii, E., Ogihara, H., Kim, D. K., Ito, A., Oboki, K., Lee, Y. M., Jippo, T., Nomura, S., Maeyama, K., Lamoreux, M. L., and Kitamura, Y. (2001) *Blood* **97,** 2038–2044
37. Kim, D. K., Morii, E., Ogihara, H., Hashimoto, K., Oritani, K., Lee, Y. M., Jippo, T., Adachi, S., Kanakura, Y., and Kitamura, Y. (1998) *Blood* **92,** 1973–1980
38. Murakami, H., and Arnheiter, H. (2005) *Pigm. Cell Res.* **18,** 265–277
39. So, H., Rho, J., Jeong, D., Park, R., Fisher, D. E., Ostrowski, M. C., Choi, Y., and Kim, N. (2003) *J. Biol. Chem.* **278,** 24209–24216
40. Mansky, K. C., Marfatia, K., Purdom, G. H., Luchin, A., Hume, D. A., and Ostrowski, M. C. (2002) *J. Leukocyte Biol.* **71,** 295–303
41. Kornak, U., Kasper, D., Bosl, M. R., Kaiser, E., Schweizer, M., Schulz, A., Friedrich, W., Delling, G., and Jentsch, T. J. (2001) *Cell* **104,** 205–215
42. Campos-Xavier, A. B., Saraiva, J. M., Ribeiro, L. M., Munnich, A., and Cormier-Daire, V. (2003) *Hum. Genet.* **112,** 186–189
43. Ramirez, A., Faupel, J., Goebel, I., Stiller, A., Beyer, S., Stockle, C., Hasan, C., Bode, U., Kornak, U., and Kubisch, C. (2004) *Hum. Mutat.* **23,** 471–476
44. Lange, P. F., Wartosch, L., Jentsch, T. J., and Fuhrmann, J. C. (2006) *Nature* **440,** 220–223
45. Cassady, A. I., Luchin, A., Ostrowski, M. C., and Hume, D. A. (2003) *J. Bone Miner. Res.* **18,** 1901–1904
46. Luchin, A., Suchting, S., Merson, T., Rosol, T. J., Hume, D. A., Cassady, A. I., and Ostrowski, M. C. (2001) *J. Biol. Chem.* **276,** 36703–36710
47. Pfaffl, M. W. (2001) *Nucleic Acids Res.* **29,** e45
48. Miki, R., Kadota, K., Bono, H., Mizuno, Y., Tomaru, Y., Carninci, P., Itoh, M., Shibata, K., Kawai, J., Konno, H., Watanabe, S., Sato, K., Tokusumi, Y., Kikuchi, N., Ishii, Y., Hamaguchi, Y., Nishizuka, I., Goto, H., Nitanda, H., Satomi, S., Yoshiki, A., Kusakabe, M., DeRisi, J. L., Eisen, M. B., Iyer, V. R., Brown, P. O., Muramatsu, M., Shimada, H., Okazaki, Y., and Hayashizaki, Y. (2001) *Proc. Natl. Acad. Sci. U. S. A.* **98,** 2199–2204
49. Stacey, K. J., Ross, I. L., and Hume, D. A. (1993) *Immunol. Cell Biol.* **71,** 75–85
50. Mizushima, S., and Nagata, S. (1990) *Nucleic Acids Res.* **18,** 5322
51. Aksan, I., and Goding, C. R. (1998) *Mol. Cell. Biol.* **18,** 6930–6938
52. Mansky, K. C., Sulzbacher, S., Purdom, G., Nelsen, L., Hume, D. A., Rehli, M., and Ostrowski, M. C. (2002) *J. Leukocyte Biol.* **71,** 304–310
53. Oddie, G. W., Schenk, G., Angel, N. Z., Walsh, N., Guddat, L. W., de Jersey, J., Cassady, A. I., Hamilton, S. E., and Hume, D. A. (2000) *Bone* (*NY*) **27,** 575–584
54. Halleen, J. M., Raisanen, S., Salo, J. J., Reddy, S. V., Roodman, G. D., Hentunen, T. A., Lehenkari, P. P., Kaija, H., Vihko, P., and Väänänen, H. K. (1998) *Bone* (*NY*) **23,** W108
55. Mitic, N., Valizadeh, M., Leung, E. W., de Jersey, J., Hamilton, S., Hume, D. A., Cassady, A. I., and Schenk, G. (2005) *Arch. Biochem. Biophys.* **439,** 154–164
56. Saftig, P., Hunziker, E., Wehmeyer, O., Jones, S., Boyde, A., Rommerskirch, W., Moritz, J. D., Schu, P., and von Figura, K. (1998) *Proc. Natl. Acad. Sci. U. S. A.* **95,** 13453–13458
57. Gelb, B. D., Shi, G.-P., Chapman, H. A., and Desnick, R. J. (1996) *Science* **273,** 1236–1238
58. Gowen, M., Lazner, F., Dodds, R., Kapadia, R., Feild, J., Tavaria, M., Bertoncello, I., Drake, F., Zavarselk, S., Tellis, I., Hertzog, P., Debouck, C., and Kola, I. (1999) *J. Bone Miner. Res.* **14,** 1654–1663
59. Kasper, D., Planells-Cases, R., Fuhrmann, J. C., Scheel, O., Zeitz, O., Ruether, K., Schmitt, A., Poet, M., Steinfeld, R., Schweizer, M., Kornak, U., and Jentsch, T. J. (2005) *EMBO J.* **24,** 1079–1091
60. Henriksen, K., Gram, J., Schaller, S., Dahl, B. H., Dziegiel, M. H., Bollerslev, J., and Karsdal, M. A. (2004) *Am. J. Pathol.* **164,** 1537–1545
61. Chalhoub, N., Benachenhou, N., Rajapurohitam, V., Pata, M., Ferron, M., Frattini, A., Villa, A., and Vacher, J. (2003) *Nat. Med.* **9,** 399–406

The Expression of *Clcn7* and *Ostm1* in Osteoclasts Is Coregulated by Microphthalmia Transcription Factor

Nicholas A. Meadows, Sudarshana M. Sharma, Geoffrey J. Faulkner, Michael C. Ostrowski, David A. Hume and Alan I. Cassady

J. Biol. Chem. 2007, 282:1891-1904.
doi: 10.1074/jbc.M608572200 originally published online November 14, 2006
